Vortex phases in superconducting Nb thin films with periodic pinning

J. E. Villegas,[1,*] E. M. Gonzalez,[1] Z. Sefrioui,[2] J. Santamaria,[2] and J. L. Vicent[1]
[1]*Departamento de Física de Materiales, Facultad de Ciencias Físicas, Universidad Complutense de Madrid, 28040 Madrid, Spain*
[2]*GFMC, Departamento de Física Aplicada III, Facultad de Ciencias Físicas, Universidad Complutense de Madrid, 28040 Madrid, Spain*

(Received 8 June 2005; revised manuscript received 4 August 2005; published 16 November 2005)

Magnetotransport properties have been used to investigate vortex phases in Nb films with periodic arrays of magnetic pinning centers. This kind of samples show a continuous glass transition similar to that observed in Nb plain films, but the periodic pinning yields different critical exponents and enhanced glass transition temperature at the matching field.

DOI: 10.1103/PhysRevB.72.174512 PACS number(s): 74.78.−w, 74.25.Dw, 74.25.Qt

Phase transitions in vortex matter is one of the most interesting research topics, as shown by the flood of papers published during recent years. The phenomenology of vortex phases is especially rich in the case of high critical temperature superconductors (HTCS),[1] because of the larger anisotropy and thermal fluctuations. Nevertheless, different vortex phases have also been observed in low critical temperature superconductors (LTCS), including vortex *liquid* and different vortex *solid* phases (as the vortex-glass[2–4] or the novel Bragg-glass[5,6]). Disorder plays a crucial role in determining which of those phases is stabilized. While materials with weak or no disorder exhibit an Abrikosov vortex-lattice with long-range topological order, random pinning or thermal fluctuations stabilize a Bragg-glass phase with quasi-long-range topological order.[5] The statics of vortex-lattices has been extensively investigated and it is known that a Bragg-glass undergoes a transition into a disordered vortex-glass[2] or a pinned liquid upon increase of disorder or field,[5] while a different Bose-glass[7,8] may develop in the presence of columnar defects. In Nb single crystals, small angle neutron data have indicated Bragg-glass *melting* (disordering).[6] In Nb thin films, on the other hand, the logarithmic time decay of the remanent magnetization below the irreversibility line suggested a *melting* transition of the vortex-lattice,[9] while the negative curvature at low currents of E-J isotherms[10] or their scaling behavior[4] have been discussed to point to the existence of a glass transition. Furthermore aging and memory effects, characteristic of glassy dynamics, have been recently reported by Sun *et al.* in Nb films covered by a disordered array of magnetic nanoparticles.[11] Despite the static properties of the vortex-lattice being largely investigated an open question is how moving lattices (for example under the action of a driving current) will behave, and how the glassy properties of the static system will be affected by lattice motion. It has been argued that at large vortex velocities disorder would produce little effect since the pinning force on a single vortex varies rapidly.[12] On the other hand Giamarchi *et al.*[13] favor the picture of a moving glass, i.e., glassy properties remain in moving lattices.

Most of the experimental studies so far have considered the effect of random disorder. Nanolithography techniques allow fabricating ordered arrays of pinning centers,[14] so that the interaction of vortices with an *in-plane* periodic distribution of defects can be studied. Such interaction yields dramatic effects, such as guided vortex motion[15] or the ratchet effect.[16] These effects are related to vortex pinning enhancement due to the matching of the vortex density to the density of pinning sites.[17] It has been shown experimentally that such commensurability effects depend strongly on the vortices velocity, suggesting that the interaction between vortices and pinning centers could be dynamically tuned and yield different degrees of topological order of the vortex-lattice.[18] Also numerical simulations for samples with periodic pinning showed that transitions between different ordering states of the vortex-lattice can be dynamically triggered.[19] Besides, simulations suggested that in the static situation *melting* of the vortex-lattice occurs at a higher temperature than in pin free systems.[19] In this paper we address experimentally which are the vortex phases in Nb samples with periodic pinning, and how they are affected by the relative intensity of random (native) to periodic pinning. To this end we have used a scaling approach of dc I-V characteristics that allows their collapse in terms of several critical exponents. We applied such analysis to a Nb film on top of a periodic array of magnetic dots, and compared with the results for a Nb plain film. The scaling of the I-V characteristics found for both types of samples, together with some additional criteria,[20] indicate the existence of a second-order continuous phase transition separating a glass phase with long-range superconducting phase coherence (zero-resistance) from a dissipative vortex-liquid. Such scaling behavior is compatible either with the existence of a vortex-glass[2] or a different Bose-glass.[7] As we show later, we cannot distinguish between the former or the latter from scaling arguments. In any case, the existence of a glass state suggests that long-range topological order is frustrated, despite the presence of periodic pinning and commensurability effects, because of the interplay with the coexisting strong random pinning (native). Periodic pinning yields two effects on the glass transition. On one hand, the critical exponents are different than in the plain film. On the other hand, the glass transition is moved up at the matching field, i.e., the glass transition temperature is higher at the matching field than at the lower but out-of-matching field. We will explain within this frame work the dependence of commensurability effects on vortex velocity and relate it to the dynamic properties of the glass phase.

Samples were prepared using a combination of e-beam lithography and sputtering techniques. Details on sample

TABLE I. The vortex-glass scaling parameters of some of the samples A and B.

			Scaling parameters				
Sample	T_c (K)	H (Oe)	T_g (K)	T_g/T_c	D	z	ν
A	8.264	85	8.194	0.9915	3	4.2	1.6
		170	8.152	0.9864	3	4.2	1.6
B	8.210	60	8.139	0.9913	3	5.9	1.0
		82	8,147	0.9923	3	5.7	1.0
		165	8.129	0.9901	3	4.2	1.0

fabrication can be found elsewhere.[14] Sample A was a 100 nm thick Nb plain film, and sample B was a 100 nm thick Nb film on top of a square array of magnetic Ni dots. The array lattice spacing was a=500 nm, the Ni dots height was 40 nm and their diameter was $\varnothing$=200 nm. Samples were lithographed with a standard four-probe configuration measuring bridge 40 μm long and 40 μm wide. Magnetotransport measurements were carried out in a liquid He cryostat that allowed controlling temperature with stability of 1 mK. The magnetic field H was always applied perpendicular to the film plane. The critical temperatures T_c are listed in Table I.

In Fig. 1(a) it is shown the dc magnetoresistance as a function of the applied field H of sample B. The curve shows periodic minima at fields H=nH_m, where n is an integer and H_m=82 Oe. This matching field is in good agreement with the one expected[17] for this array $H_m=\phi_0/a^2$=82.9 Oe, with $\phi_0=2.07\cdot10^{-15}$ Wb and a=500 nm. Figure 1(b) shows dc I-V characteristics at temperatures $t_A=0.997T_c$ (triangles) and $t_B=0.989T_c$ (circles), for two different applied magnetic fields H_{out}=60 Oe (black symbols) and H_m=82 Oe (white symbols), out and at the first matching field respectively. Characteristics measured at higher temperature (t_A) show ohmic resistance at low current levels. This linear response holds up to a given current level I_{nl}, above which the curves deviate from linearity and show positive curvature (increasing slope). Characteristics at lower temperature (t_B), on the other hand display a completely different behavior. They are nonlinear in the whole experimental window and display negative curvature, showing zero resistance in the low current limit $\lim_{I\to0} V/I=0$. The effect of commensurability can be clearly seen for both temperatures: in the two cases characteristics for the matching field H_m shifts to higher currents with respect to those at H_{out}, i.e., for all current levels the resistance is lower for H_m than for H_{out}.

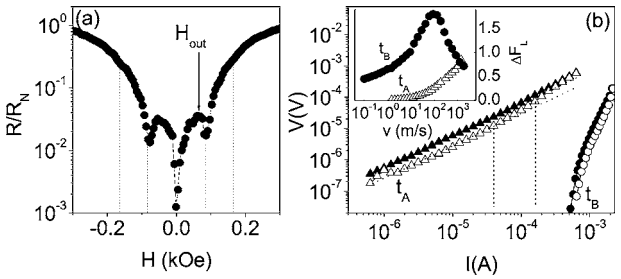

FIG. 1. (a) A magnetoresistance of sample B at T=0.995 T_c, with J=12.5 kA$\cdot$cm^{-2}. The vertical dashed lines point to matching fields. (b)The I-V characteristics at $t_A=0.997$ T_c (triangles) and $t_B=0.989$ T_c (circles). The black symbols are for H=60 Oe(H_{out}) and the white symbols are for H=82 Oe (H_m, first matching). Insert: The pinning enhancement at the matching field $\Delta F_L(v)$ [in 10^{-7} N$\cdot$m^{-1}] for t_A (white symbols) and t_B (black symbols).

The pinning force enhancement at the matching field can be obtained from I-V curves.[18] We calculated the vortex-lattice velocity v and the Lorentz force on the vortex-lattice, F_L. Using the expression for the electric field $\vec{E}=\vec{B}\times\vec{v}$ (where $\vec{B}$ is the applied magnetic field and $\vec{v}$ the vortex-lattice velocity), we obtained $v=V/(dB)$ (where V is the voltage and d the distance between contacts). For the Lorentz force we used $\vec{F}_L=\vec{J}\times\vec{n}\phi_0$ (where J is the injected current density and $\vec{n}$ a unitary vector parallel to the applied magnetic field). Thus, we calculated $F_{L\,m}(v)$ and $F_{L\,out}(v)$ from the corresponding I-V characteristics. The difference gives the pinning force enhancement at the matching field as a function of the vortex-lattice velocity

$$F_{Lm}(v)-F_{Lout}(v)\equiv\Delta F_L(v). \tag{1}$$

We applied this analysis to those characteristics shown in Fig. 1(b). Different behavior is found for the two temperatures t_A and t_B as shown in the inset of Fig. 1(b). For the lower temperature (t_B) the pinning force enhancement $\Delta F_L(v)$ peaks at intermediate vortex-lattice velocities around $v\sim100$ m/s. This is in agreement with the results reported earlier for other array geometries and sizes.[18] For the higher temperature (t_A), on the contrary, $\Delta F_L(v)$ increases monotonically as the vortex-lattice velocity increases. Besides, the pinning enhancement for this temperature is comparatively smaller, and only at high vortex-lattice velocities its value is comparable to that observed for lower temperatures. We show below that the different dynamical evolution of the pinning force enhancement for the two temperatures t_A and t_B is related to the different vortex phases being stabilized.

We measured several sets of isothermal dc I-V characteristics for samples A and B, at several applied magnetic fields. For each sample and field, the corresponding set contained $\sim$20 I-V characteristics. Data of sample A, the Nb plain film, are published elsewhere.[4] Some of the data of sample B are collected in Fig. 2(a) and in Fig. 3(a). We applied to those I-V characteristics the scaling analysis proposed by Fisher *et al.*[2] in the theory of the vortex-glass transition. In the vicinity of this continuous transition, i.e., in the critical region close to the glass transition temperature T_g, the relevant physical magnitudes scale with the vortex-glass correlation length ξ_{VG} and a relaxation time $\tau\cdot\xi_{VG}$ and τ diverge as temperature approaches T_g, as $\xi_{VG}\propto(T-T_g)^{-\nu}$ and $\tau\propto(T-T_g)^{-z\nu}$, where z and ν are the dynamic and the static critical exponents respectively. Following the theory, I-V characteristics should scale down with the ansatz

$$E\xi_{VG}\tau\approx J\xi_{VG}^{D-1}\zeta_{\pm}(J\phi_0\xi_{VG}^{D-1}/k_BT), \tag{2}$$

where E is the electric field, J the current density, D is the dimensionality of the glass transition (D=3 for a three-dimensional superconductor), $\zeta_{\pm}$ is a universal scaling function above (ζ_+) or below (ζ_-)T_g, and k_B the Boltzmann con-

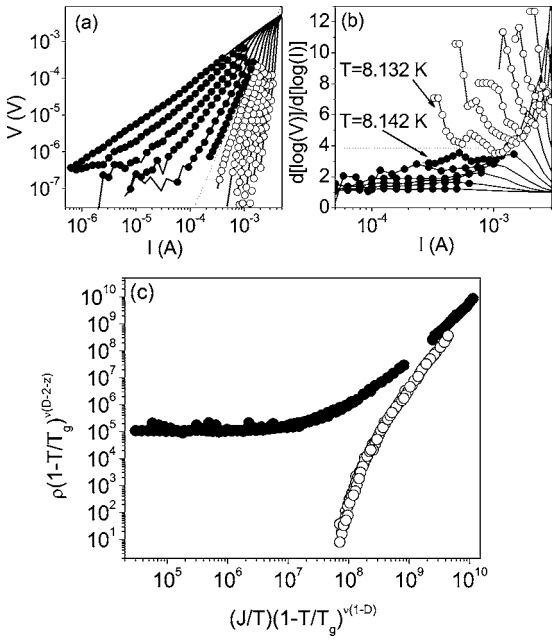

FIG. 2. (a)The I-V isotherms for sample B in applied field H=60 Oe, separated ~10 mK. The dots are data points used for scaling analysis; the black ones are for isotherms at $T > T_g$ and the white ones for $T < T_g$. (b) Derivatives of the log(V)- log(I) curves. Derivatives for isotherms around $T_g = 8.139$ are marked with arrows and separated by a horizontal dotted line. (c) Scaling of the above isotherms as explained in the text.

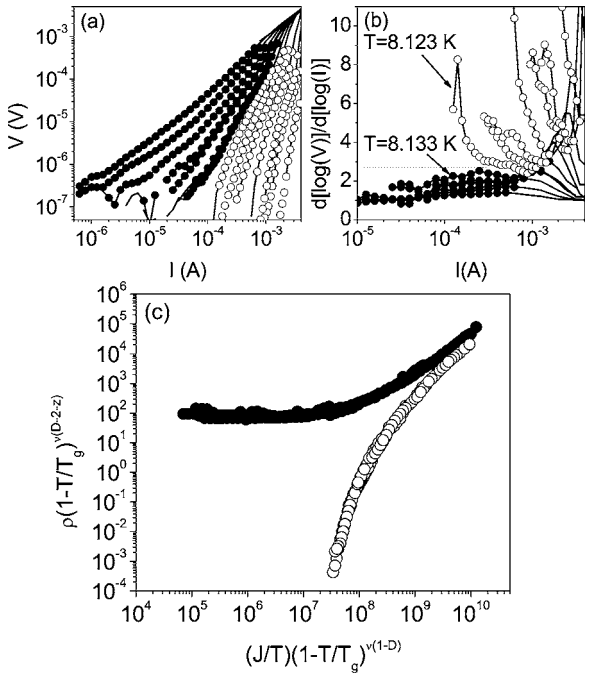

FIG. 3. (a) The I-V isotherms for sample B in applied field H=165 Oe, separated ~10 mK. The dots are data points used for scaling analysis; the black dots are for isotherms at $T > T_g$ and the white dots are for $T < T_g$. (b) Derivatives of the log(V)- log(I) curves. Derivatives for isotherms around $T_g = 8.129$ are marked with arrows and separated by the horizontal dotted line. (c) Scaling of the above isotherms are explained in the text.

stant. The scaling was successful for any set of I-V characteristics measured for samples A and B. As an example of the obtained results, collapses of the isotherms shown in Fig. 2(a) and Fig. 3(a) are displayed in Fig. 2(c) and Fig. 3(c) respectively. The resistivity is $\rho = E/J$. E and J were calculated from V and I using the measuring bridge dimensions and samples thickness. Only data within the experimental window $V \lesssim 5 \cdot 10^{-4}$ V were used since, above this cut-off voltage, the currents injected were too high and drove the system towards free flux flow, where the scaling analysis is no longer valid.[20] The dimensionality was always D=3. Attempts to use D=2 did not allow collapsing any set of characteristics. The parameters T_g, z, and ν are listed on Table I for several fields and also for sample A (taken from Ref. 4). The experimental values of the critical exponents are in the range $z \approx 4-6$ and $\nu \approx 1-2$ predicted by the theory.

The scaling relation proposed in the Bose-glass theory[7] resembles formally that of the vortex-glass (Eq. (2)), although the theories themselves differ in a number of important ways. In the Bose-glass theory there are two different diverging characteristics lengths, the localization length $l_\perp \propto (T - T_g)^{-\nu'}$ and the correlation length along the vortex line $l_\parallel \propto l_\perp^{z'}$, and a different relaxation time $\tau \propto l_\perp^{z'}$. However, if the scaling of the isotherms is achieved through (Eq. (2)) with D=3 and vortex-glass critical exponents z and ν, then automatically the scaling is also obtained for the Bose-glass model but with exponents $z' = 1/2(3z+1)$ and $\nu' = \frac{2}{3}\nu$.[21] I.e., vortex-glass and Bose-glass cannot be distinguished from scaling arguments. For the sample with periodic pinning, the Bose-glass picture might be more likely than the vortex-glass one. It has been experimentally shown[17,22] for this kind of sample that in the temperature and field ranges relevant to our experiments, magnetotransport properties depend only on the component of the magnetic field perpendicular to the film plane, because the penetration length λ is comparable to sample thickness.[22] I.e. at a given temperature, the resistance in a field H applied at any angle θ with respect to the film plane is the same than the resistance in a field $H' = H \sin(\theta)$ applied perpendicular to the film plane.[22] This favors a picture in which the magnetic dots act as extended defects, promoting flux-line localization along the direction perpendicular to the film plane and inhibiting vortex wandering.

We want to note at this point that the above scaling analysis has been subject of controversy recently. It was shown that, for a given set of I-V curves, different combinations of the values of T_g and the critical exponents z, ν provide collapses of similar quality, essentially depending on the voltage sensitivity floor,[20] thus questioning the use of the scaling of I-V characteristic as a direct evidence of a zero-resistance glass phase. In Ref. 20 it was argued that, in order to ensure the existence of a truly superconducting state with the above analysis and unambiguously determine T_g, the experimental data must fulfill the following criterion: in the low-current limit, isotherms at the same reduced temperature $|(T - T_g)/T_g|$ above and below T_g must have opposite curvature at the same current level. We have used this criterion to confirm the values of T_g obtained from the scaling procedure for each set of I-V characteristics. This was checked using

the derivatives $d[\log(V)]/d[\log(I)]$. Some examples of them are shown in Fig. 2(b) and 3(b). Isotherms measured at $T > T_g$ (black circles) and at $T < T_g$ (white circles) have opposite curvatures in the low-current limit, since derivatives go downward (decreasing slope) and upward (increasing slope) respectively as current is decreased. In particular, for the isotherms of Fig. 2(a) the scaling analysis yielded $T_g = 8.139$ K. As can be seen in Fig. 2(b) in the low-current limit the isotherms just above T_g(T=8.142 K) and just below (T=8.132 K) have opposite curvatures at equal current levels. The same can be checked for isotherms in Figs. 3(a) and 3(b), for which $T_g = 8.129$ K.

We have also used those derivatives to check the values of the critical exponents obtained from the scaling procedure. The critical isotherm (the one at $T = T_g$) must fulfill[2] $E \propto J^{\alpha+1}$, where $\alpha = (z+2-D)/(D-1)$. Therefore, for such an isotherm $d[\log(V)]/d[\log(I)] = \alpha + 1$. The exact critical isotherm was not measured but, using the derivatives of the isotherms just above and below T_g, we estimated the upper and lower limits of $\alpha+1$. In particular, from Fig. 2(b) we obtained $3.6 < \alpha + 1 < 4.1$, that together with D=3 yielded $5.2 < z < 6.2$. The value obtained from the scaling, $z = 5.9 \pm 0.1$, was well within that range. For the data in Fig. 3(b) $2.5 < \alpha + 1 < 3.0$, and therefore the critical exponent must be $4.0 < z < 5.0$. This is also in good agreement with the value obtained from the scaling $z = 4.2 \pm 0.1$.

The values of the critical exponents (see Table I) and their field dependence are different for the plain films (sample A) and for the nanostructured (sample B). The critical exponents for sample A do not depend on the applied magnetic field. For sample B, on the contrary, different critical exponents are obtained below and above the first matching field. While $\nu \sim 1$ always, $z \sim 5.8$ below and at the first matching field (H=60 Oe and H=82 Oe) and $z \sim 4.2$ in the second matching field H=164 Oe. This change may be related to the appearance of interstitial vortices above the first matching field. In any case, the critical exponents for sample B are different to those for Nb plain film, showing that the presence of the periodic pinning is affecting the dynamic of the glass transition. But the most interesting feature is that the glass transition temperature T_g is enhanced at the first matching field. Thus, when going from H=60 Oe to H=82 Oe, T_g increases from $T_g = 8.139$ K to $T_g = 8.147$ K, contrary to what should happen in the absence of periodic pinning. This signature of the matching is different to that found earlier in HTCS with columnar defects, where a change in the slope dT_g/dH (but not an enhancement of T_g) was observed at the first matching field.[23] However, the experimental situation of Ref. 23 is rather different, since the columnar defects are correlated along the vortex line but *randomly* distributed in-plane. Our experiment shows that the existence of a *in-plane* periodic distribution of pinning centers moves up the transition from the liquid into the glass state. In other words, the presence of periodic pinning enhances glass correlation lengths. This commensurability effect, additional to the enhancement of vortex pinning in the glass phase, makes possible that even the linear (ohmic) magnetoresistance (at high temperature and low injected currents) shows up the signature of the matching, i.e., minima at fields $H = nH_m$.

The experimental results shown so far evidence that vortex matter undergoes a second order glass transition separating a liquid phase from a glass phase at lower temperatures, both in plain and nanostructured Nb thin films. This rules out the possibility of the low temperature phase being a true Bragg-glass,[13] for which a first order (instead of second order) transition into a liquid would be expected.[6] A true Bragg-glass is indeed not likely in Nb plain films, because of the strong random pinning. On the contrary, for the sample with periodic (*ordered*) pinning centers, one might foresee a long-range or quasi-long-range topologically ordered vortex phase, provided the observable commensurability effects. However, the scaling results found here suggest that the coexisting random pinning frustrates the long-range topological order of the vortex-lattice, yielding instead a glass phase. The resulting picture could be that, at the matching fields, geometrical coincidence between the vortex-lattice and the periodic array of pinning centers takes place in regions (*domains*) of finite size. The vortex-lattice would be ordered matching the symmetry of the periodic potential within such domains, say within a length scale ξ_t. But such ordering would be lost beyond the boundaries of the domains, because some vortices eventually accommodate in (or are attracted to) disordered intrinsic pinning sites that are stronger than the artificial ones. In this way long-range order is frustrated and glassy properties result of a short-range Bragg-glass with topological order decaying over the length scale ξ_t, as recently suggested by Giamarchi and Le Doussal.[13] The stronger is periodic pinning as compared to random, the more pronounced commensurability effects and the larger ξ_t, and *vice versa*.

The dynamical evolution of the pinning enhancement $\Delta F_L(v)$ at the matching field can be explained within this picture. In Fig. 1(b), the curves at higher temperature (t_A) are measured above the glass transition temperature. For that temperature $\Delta F_L(v)$ is small, especially at low vortex velocities [see the insert of Fig 1(b)]. Low velocities are achieved at low current levels, i.e., in the ohmic regime of the I-V characteristics, where the response of the vortex-liquid is being probed. As the vortices velocity is increased, $\Delta F_L(v)$ increases monotonically. This is because the higher current level needed to drive vortices at higher velocities corresponds to the nonlinear regime of the I-V curves, in which pinning is being probed. On the other hand the curve corresponding to the temperature t_B (below the glass transition temperature T_g) shows a different behavior [see the insert of Fig 1(b)]. $\Delta F_L(v)$ is larger at all velocities, and shows a peak around $v \sim 100$ m/s. It has been theoretically shown[12] that the disturbing effect of the pinning forces on the vortex-lattice vanishes as velocity increases. The behavior of $\Delta F_L(v)$ can be explained[18] considering the two different kinds of pinning coexisting in our system, random (native) and periodic. At low vortex velocities, below the maximum of $\Delta F_L(v)$, random pinning is gradually overcome as velocity is increased and therefore periodic pinning becomes dominant. In this regime commensurability effects get more pronounced [$\Delta F_L(v)$ increases], which indicates an increase of the order characteristic length ξ_t. This trend holds up to a given velocity, above which the effect of periodic pinning

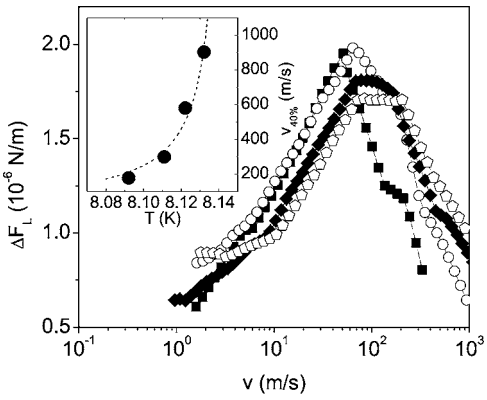

FIG. 4. The pinning enhancement at the matching field $\Delta F_L(v)$ for several temperatures T=8.132 K (white pentagons), T=8.122 K (black diamonds), T=8.111 K (white circles), and T=8.092 K (black squares). Insert: The velocity at which $\Delta F_L(v)$ has decreased 40 % from maximum, $v_{40\%}$, as a function of temperature. The dashed line is the best fit to $v_{40\%} \propto 1/(\mathbf{T}_{eff}-\mathbf{T})$, as explained in the text.

starts being overcome. Thus, from the point at which $\Delta F_L(v)$ reaches its maximum value, further increase of velocity leads to a reduction of commensurability effects [$\Delta F_L(v)$ decreases]. It is expected that at higher vortex velocities, once the effects of all pinning mechanisms have been washed out, the vortex-lattice recovers its *natural* order and becomes a moving crystal.[12,19]

We show several more $\Delta F_L(v)$ curves for temperatures $T<T_g$ in Fig. 4. All of them display similar shape, with a maximum around $v \sim 50$-100 m/s. Curves shift to the left (lower velocities) as temperature is decreased. This behavior is consistent (see above) with the distortions induced by the pinning potential vanishing as the vortex-lattice velocity increases. In particular, the temperature dependence suggests that the effect of disorder can be understood in terms of an effective shaking temperature T_{sh} that decreases with vortex velocity, $T_{sh} \propto 1/v$.[12] If one assumes that all pinning mechanisms are overcome at an effective energy scale described by an effective temperature $T_{eff}=T+T_{sh}$, the shifting of $\Delta F_L(v)$ to lower velocities should be described by $v \propto 1/(T_{eff}-T)$. This is roughly the temperature dependence observed, as shown in the inset of Fig. 4. We have plotted the velocity at which $\Delta F_L(v)$ has decreased 40 % from its maximum value,[24] $v_{40\%}$, as a function of temperature T. The dashed line is the best fit to the thermal expected dependence $v \propto 1/(\mathbf{T}_{eff}-\mathbf{T})$, which yielded $T_{eff}=8.14\pm0.02$ K.

In summary, using a scaling analysis of I-V characteristics, we have found that Nb thin films with periodic arrays of magnetic pinning centers show a continuous glass transition, similar to that observed in plain Nb films. In nanostructured samples, the random and periodic pinning mechanism coexisting compete and yield a glass phase which does not present long-range topological order. Two remarkable commensurability effects are present in the transport properties. (i) In the critical region above the glass phase, glass correlation lengths are enhanced at the matching fields, yielding a higher glass transition temperature T_g. Because of this, reduced dissipation at the matching fields can be observed even in the ohmic regime. (ii) In the glass phase, vortex pinning is enhanced at the matching fields. This pinning enhancement depends on vortex velocity, as the relative intensity of random versus periodic pinning is dynamically tuned.

We would like to thank the Spanish Ministerio de Educación y Ciencia for support under Grant Nos. MAT202-04543 and MAT2002-12385-E, CAM under Grant No. GR/MAT/0617/2002, and the "Ramón Areces" Foundation. One of us, E.M.G., wants to thank the Spanish Ministerio de Educación y Ciencia for a "Ramón y Cajal" contract.

*Present address: Physics Department, University of California, San Diego, La Jolla, CA 92093-0319, USA

[1] F. Bouquet, C. Marcenat, E. Steep, R. Calemczuk, W. K. Kwok, U. Welp, G. W. Crabtree, R. A. Fisher, N. E. Phillips, and A. Schilling, Nature (London) **411**, 449 (2001).
[2] D. S. Fisher, M. P. A. Fisher, and D. A. Huse, Phys. Rev. B **43** 130 (1991).
[3] S. Okuma and N. Kokubo, Phys. Rev. B **56**, 14138 (1997).
[4] J. E. Villegas and J. L. Vicent, Phys. Rev. B **71**, 144522 (2005).
[5] T. Giamarchi and P. Le Doussall, Phys. Rev. Lett. **72**, 1530 (1994).
[6] S. R. Park, S. M. Choi, D. C. Dender, J. W. Lynn, and X. S. Ling, Phys. Rev. Lett. **91**, 167003 (2003).
[7] D. R. Nelson and V. M. Vinokur, Phys. Rev. Lett. **68**, 2398 (1992).
[8] W. Jiang, N.-C. Yeh, D. S. Reed, U. Kriplani, D. A. Beam, M. Konczykowski, T. A. Tombrello, and F. Holtzberg, Phys. Rev. Lett. **72**, 550 (1994).
[9] M. F. Schmidt, N. E. Israeloff, and A. M. Goldman, Phys. Rev. Lett. **70**, 2162 (1993); Phys. Rev. B **48**, 3404 (1993).
[10] Y. Ando, H. Kubota, and S. Tanaka, Phys. Rev. B **48**, 7716 (1993).
[11] Y. Sun, M. B. Salamon, K. Garnier, and R. S. Averback, Phys. Rev. Lett. **92**, 097002 (2004).
[12] A. E. Koshelev and V. M. Vinokur, Phys. Rev. Lett. **73**, 3580 (1994).
[13] T. Giamarchi and P. Le Doussal, Phys. Rev. Lett. **76**, 3408 (1996).
[14] J. I. Martín, J. Nogués, K. Liu, J. L. Vicent, and I. K. Schuller, J. Magn. Magn. Mater. **256**, 449 (2003).
[15] J. E. Villegas, E. M. Gonzalez, M. I. Montero, I. K. Schuller, and J. L. Vicent, Phys. Rev. B **68**, 224504 (2003).
[16] J. E. Villegas, S. Savel'ev, F. Nori, E. M. Gonzalez, J. V. Anguita, R. Garcia, and J. L. Vicent, Science **302**, 1188 (2003); J. E. Villegas, E. M. Gonzalez, M. P. Gonzalez, J. V. Anguita, and J. L. Vicent, Phys. Rev. B **71**, 024519 (2005).
[17] J. I. Martín, M. Vélez, J. Nogués, and I. K. Schuller, Phys. Rev. Lett. **79**, 1929 (1997).

[18] M. Vélez, D. Jaque, J. I. Martín, F. Guinea, and J. L. Vicent, Phys. Rev. B **65**, 094509 (2002).
[19] C. Reichhardt and G. T. Zimányi, Phys. Rev. B **61**, 14354 (2000).
[20] D. R. Strachan, M. C. Sullivan, P. Fournier, S. P. Pai, T. Venkatesan, and C. J. Lobb, Phys. Rev. Lett. **87**, 067007 (2001).
[21] P. J. M. Wöltgens, C. Dekker, J. Swuste, and H. W. de Wijn, Phys. Rev. B **48**, 16826 (1993).
[22] O. M. Stoll, M. I. Montero, J. Guimpel, Johan J. Åkerman, and Ivan K. Schuller, Phys. Rev. B **65**, 104518 (2002).
[23] A. W. Smith, H. M. Jaeger, T. F. Rosenbaum,W. K. Kwok, and G. W. Crabtree, Phys. Rev. B **59**, R11665 (1999).
[24] We have used this criterion since, because of the experimental voltage cutoff $V \lesssim 5 \cdot 10^{-4}$ V, each $\Delta F_L(v)$ reaches a different minimum value within the experimental window.